



Article

Radiogenic Pb Enrichment of Mississippi Valley-Type Metallic Ore Deposits, Southern Ozarks: Constraints Based on Geochemical Studies of Source Rocks and Their Diagenetic History

Jonathan Chick ¹, Sydney E. McKim ², Adriana Potra ^{1,*} , Walter L. Manger ¹ and John R. Samuelsen ³ 

¹ Department of Geosciences, University of Arkansas, Fayetteville, AR 72701, USA; jchick@uark.edu (J.C.); wmanger@uark.edu (W.L.M.)

² Department of Geology and Geophysics, University of Wyoming, Laramie, WY 82071, USA; smckim3@uwyo.edu

³ Arkansas Archeological Survey, University of Arkansas, Fayetteville, AR 72704, USA; jsamuel@uark.edu

* Correspondence: potra@uark.edu

Abstract: Southern Ozark Mississippi Valley-type ores are enriched in radiogenic Pb, with isotopic signatures suggesting that metals were supplied by two end-member components. While the less radiogenic component appears to be derived from various shale and sandstone units, the source of the more radiogenic component has not yet been identified. Analyses of cherts from the Early Ordovician Cotter Dolomite and tripolitic chert from the Early Mississippian Boone Formation contain highly radiogenic Pb, with isotopic ratios comparable to those of ores. However, most samples have lower $^{208}\text{Pb}/^{204}\text{Pb}$ and $^{207}\text{Pb}/^{204}\text{Pb}$ for a given $^{206}\text{Pb}/^{204}\text{Pb}$ compared to ores. These relationships demonstrate that the enriched Pb isotopic values of the ore array cannot be related to the host and regional lithologies sampled, suggesting that the source of high ratios may lay further afield. The slope of the linear trend defined by the Pb isotope ratios of ores corresponds to an age of about 1.19 Ga. Therefore, an alternative for the linear array is the involvement of Precambrian basement in supplying ore Pb. Rare earth element patterns show that diagenetic processes involving the action of groundwater and hydrothermal fluids affected the sampled lithologies to various degrees, with Cotter Dolomite having experienced the highest degree of alteration.

Keywords: Mississippi Valley-type ores; Ozark region; tripolitic chert; Pb isotopes; rare earth elements



Citation: Chick, J.; McKim, S.E.; Potra, A.; Manger, W.L.; Samuelsen, J.R. Radiogenic Pb Enrichment of Mississippi Valley-Type Metallic Ore Deposits, Southern Ozarks: Constraints Based on Geochemical Studies of Source Rocks and Their Diagenetic History. *Geosciences* **2021**, *11*, 172. <https://doi.org/10.3390/geosciences11040172>

Academic Editors: Suzanne Golding and Jesus Martinez-Frias

Received: 29 December 2020

Accepted: 7 April 2021

Published: 10 April 2021

Publisher's Note: MDPI stays neutral with regard to jurisdictional claims in published maps and institutional affiliations.



Copyright: © 2021 by the authors. Licensee MDPI, Basel, Switzerland. This article is an open access article distributed under the terms and conditions of the Creative Commons Attribution (CC BY) license (<https://creativecommons.org/licenses/by/4.0/>).

1. Introduction

It has been hypothesized that Ordovician, Mississippian, and younger carbonate and clastic formations found within the Ouachita Uplift of west-central Arkansas, and northward onto the Ozark Dome, experienced interaction with hydrothermal fluids due to tectonic forces that caused the Ouachita Orogeny [1–3]. Geochemical studies indicate that the Mississippi Valley-type (MVT) ores were produced from a mixing and cooling of these sedimentary, basinal brines by associated meteoric or connate waters [4]. Previous investigations of the mid-continent MVT Pb and Zn mineralization (Figure 1) have been conducted, resulting in a large amount of geological and geochemical data, as well as numerous theories as to the source of the MVT ore metals and mineralizing fluids [5–10]. In the Ozark region, the linear trend defined by the Pb isotope compositions of the MVT ores suggest their formation involved a mixing of metals from two end-member components [7–10]. One end-member must have been highly radiogenic with Pb isotope ratios equal or higher than the highest measured value in the ores. The other end-member must have been less radiogenic, with Pb isotope ratios equal or lower than the lowest measured value. Extensive geochemical studies of rocks from the southern Ozark region and the Ouachita Mountains (Figure 1) have been carried out in order to constrain the two end-member components in the ores from the Northern Arkansas and the Tri-State

districts: the Devonian and Mississippian shales of the Ozark Plateaus [9], the Ordovician and Carboniferous shales and sandstones of the Ouachita Mountains [10], the various cherts from the Devonian-Lower Mississippian Arkansas Novaculite [11,12], and from the Lower Mississippian Boone Formation (the lower Boone penecontemporaneous chert and the upper Boone tripolitic and diagenetic chert) [13,14]. While the less radiogenic component has been generally attributed to various shale and sandstone units [9,10], the more radiogenic component has not yet been identified. Whole-rock Pb isotope analyses conducted for this study may help better constrain the more radiogenic component that contributed Pb to the ores. Rare earth element (REE) analyses have also been carried out on these whole-rock samples to shed light on the depositional environment and the diagenetic processes that might have affected them.

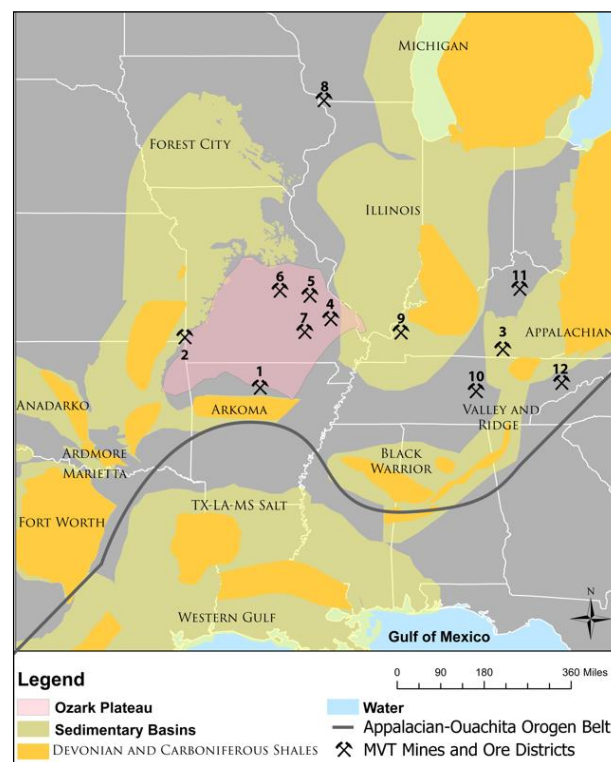


Figure 1. Map of the United States midcontinent region showing the location of sedimentary basins, shale plays, and major MVT mining districts and deposits (1 through 12): (1) Northern Arkansas, (2) Tri-State, (3) Burkesville deposit, (4) Old Lead Belt, (5) Southeast Missouri Barite, (6) Central Missouri Barite, (7) Viburnum Trend, (8) Upper Mississippi Valley, (9) Illinois–Kentucky Fluorspar, (10) Central Tennessee, (11) Central Kentucky, and (12) Eastern Tennessee. Modified from [4,9]. For drawing this basemap: <https://www.eia.gov/maps/maps.htm> (accessed on 29 December 2020).

Lead isotopes are an excellent tracer of metal sources in hydrothermal systems. Under medium (mesothermal, around 200–400 °C) to high temperature (hypothermal, around 400–600 °C) conditions, like those encountered in hydrothermal environments, Pb is soluble [15]. Under relatively low temperature environments, Pb may be complexed with organic matter [15]. Although metal-bisulfide and organometallic complexes have been suggested, only metal-chloride complexes are considered likely base metal transporting species for MVT ore fluids [16]. A threshold of approximately 10 wt. % chlorinity in sedimentary brines has been inferred for the presence of Pb (and Zn) in sedimentary fluids at MVT ore-forming conditions [17].

Lead has a similar geochemical behavior to Cu and Zn in hydrothermal fluids [18] and it occurs in the same paragenetic stages as Zn, Cu, Ag, and Cd [19,20]. Therefore, Pb isotopes can be used to constrain the source of associated metals such as Cu and Zn. Of

particular importance are the starting composition of the hydrothermal fluid, the degree of fluid–rock interaction along fluid pathways, and the relative Pb concentrations of fluid versus wall rock or other fluids [15]. These factors can greatly influence the Pb isotope composition of the ore minerals. While Pb isotopes are not measurably fractionated by redox reactions in solution or by fluid–mineral interactions, the initial composition of the fluid can clearly experience isotopic alteration by interaction with rocks and other fluids that come into contact with the ore solution. If the mixing of hydrothermal fluids is close to the site of ore deposition, a range of Pb isotope compositions may develop, whereas if mixing occurs at a significant distance, Pb isotope homogeneity may occur [15]. Comparative Pb isotope research can help identify metal-contributing source rocks for the sulfide ores, which is critical to understanding the generation and occurrence of economic Pb–Zn deposits.

Rare earth elements are among the least soluble of the trace elements and have been shown to be relatively immobile during low-grade metamorphism, weathering, and low temperature hydrothermal alteration [21]. However, under conditions of intense tropical weathering [22] or in certain types of hydrothermal environments [23], the REE may be mobile. Additionally, carbonate alteration seems to result in greater mobility of all REE, perhaps due to CO₂ reaching concentrations high enough to stabilize complexes with elements of intermediate-high ionic potential [22]. Rare earth elements have exceptionally similar chemical properties, which make them behave coherently and display smooth patterns when normalized to a typical normalizing material (shales, mantle, or chondrites). Deviations from this behavior occur when an element in the series has a unique chemical property that affects its solubility [24], or its compatibility with the solid phase vs. the melt phase during magma cooling. Although REE are predominantly trivalent, there are two exceptions: in strongly reducing environments, Eu can occur in the +2 oxidation state, and in the presence of oxygen, Ce³⁺ is partially oxidized to Ce⁴⁺. Therefore, these elements may fractionate from the 3+ REE as a function of redox potential [25].

The unique properties of the REE have been used to study geochemical processes responsible for solid phase–melt phase fractionation and petrogenesis in general, as well as to investigate the adsorptive processes and solution complexation in seawater ([26] and additional references therein). Geochemical studies of sedimentary carbonates have been used to shed light into the multivariate processes of diagenesis, as well as the chemistry of ancient oceans [27]. The REE have a distinct distribution pattern in seawater, and this pattern may or may not be preserved in carbonate sediments and rocks, depending on their diagenetic history. Therefore, the REE distribution patterns in carbonates can shed light on the origin, depositional environments, and the syn- and post-depositional processes, including any hydrothermal alteration affecting these carbonates [27].

The samples analyzed include nodular cherts associated with Ordovician and Mississippian carbonates in the Ozark Plateau, and Ouachita Mountains of Arkansas and Oklahoma. The Ordovician samples include the Bigfork Chert (Middle–Upper Ordovician) from the Ouachita Mountains and the Cotter Dolomite (Lower Ordovician) from the Ozark Plateaus. The Mississippian samples include the tripolitic chert (Lower Mississippian) from the Boone Formation in the Ozark Plateaus. A thorough description of the tripolitic chert lithology is provided in the geologic setting section. These formations were chosen for sampling because of their stratigraphic positions along hypothesized hydrothermal fluid flow paths in relation to the tripolitic chert development (Figure 2). It is known that sedimentary basinal brine fluids have undergone up-ramp flow during the Ouachita Orogeny [1–4]. Fluid flow through confined aquifers in the Ouachita Mountains and the Ozark Plateaus is very likely. Available Pb isotopic data for samples of sphalerite ore from the Northern Arkansas and Tri-State Mining districts [9,28] and for various rock units [9–14] have been incorporated into this study for a comprehensive understanding of the MVT ores.

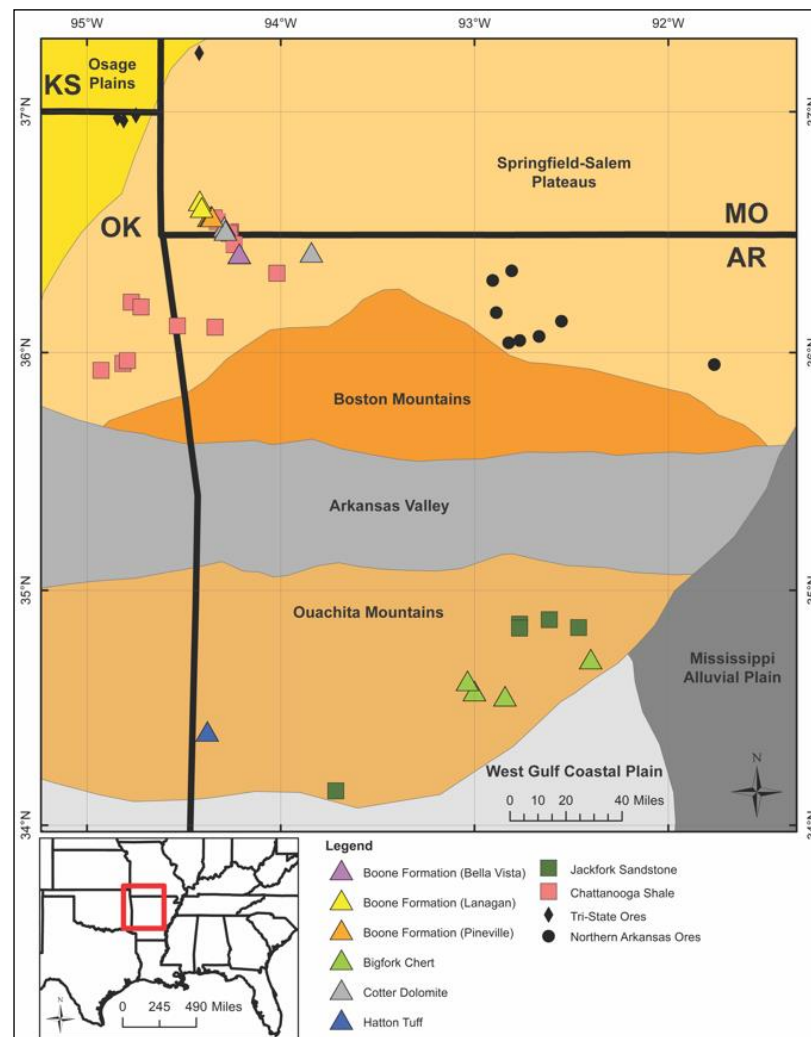


Figure 2. Location of samples analyzed in this study (triangles) and those of previous studies: squares [9,10], diamonds [9,28], and circles [9,28]. Modified from [10].

2. Geologic Setting and Mississippi Valley-Type Ores

2.1. The Ozark Plateaus

In the southern midcontinent, most of the Paleozoic section reflects eustatic cycles of transgression and regression by epeiric seas across a cratonic setting. The depositional environment is one of a relatively shallow, cratonic, continental shelf, generally sloping toward deeper oceanic settings to the south. This setting resulted in the deposition of thin lithostratigraphic units of a variety of sedimentary lithologies that dip radially away from the central Ozark Dome, a broad cratonic uplift cored by a Precambrian granite and rhyolite basement of the St. Francois Mountains [29]. The Ozark Dome is asymmetrical and consists of three plateaus: Salem, Springfield, and the Boston Mountains (Figure 2), which surround an exposed core of Precambrian granite. The lowest and northernmost of these plateaus is the Salem, which mainly exposes a succession of dolostones, sandstones, and limestones of early through late Ordovician age [30]. The Springfield Plateau exposes younger strata of Devonian through Mississippian age, capped with Pennsylvanian strata of the Boston Mountains. Each of these intervals preserves unconformity surfaces marking transgressive–regressive sea level changes as part of the Paleozoic record of the southern midcontinent.

The Ordovician Period includes the greatest global sea level highstand occurring during the Phanerozoic Eon, probably as a result of the rapid seafloor uplift in response to initial spreading along ocean ridges [31]. Lower Ordovician strata in northwestern Arkansas accumulated in a warm, shallow, epeiric sea on a broad, cratonic, and fully

aggraded platform [32]. Lower Ordovician strata of the Ozark Aquifer are primarily composed of two lithologies: dolomite and sandstone. The less permeable Cotter Dolomite (Figures 2 and 3) of the Arbuckle Group analyzed in this study is predominantly cherty dolomite with minor quartz sand beds. In the subsurface, rocks of the Arbuckle Group rest above the Late Cambrian Lamotte Sandstone, which rests unconformably on Precambrian igneous rocks [33].

The Lower Ordovician Upper Knox Dolomite in the southern Appalachian Basin is uniform in mineralogy, texture, and geochemistry over an area stretching from the Southern Appalachians to the Ozarks and Texas–Oklahoma [34]. The Lower Ordovician Cotter Dolomite (Figure 4A,B) may be genetically related to the Upper Knox Dolomite. Previous studies have concluded that there are at least three generations of dolomitization in the Upper Knox, and multiple episodes of exposure to the atmosphere related to fluctuation of sea level are the dominant mechanisms for dolomite formation rather than burial, or a single event of massive karst formation [34]. Fine-grained dolostones represent penecontemporaneous dolomitization of calcareous sediments in upper intertidal to supratidal environments [35]. Medium and coarser grained dolostones formed by early diagenetic replacement of limestones due to dilution of marine pore water by fresh water [35]. Late diagenetic dolostones record the spatial and temporal evolution of large-scale subsurface fluid migration systems that developed in response to different burial and tectonic stages of late Paleozoic Alleghenian tectonism in the southern Appalachian basin [36,37]. Zoned dolomite cements in fractures and breccias indicate that the late diagenetic dolomites likely precipitated from hot, saline brines subjected to extensive interaction with clastic lithologies, rather than as replacement [37].

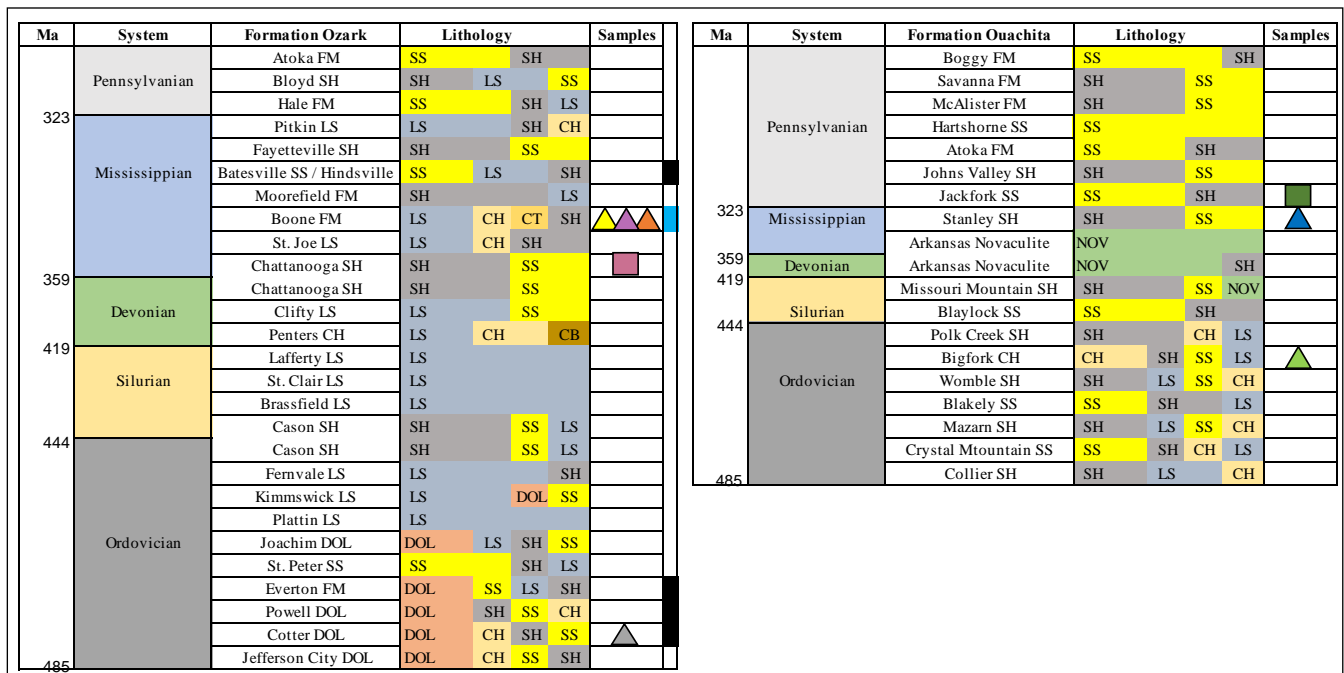


Figure 3. Generalized stratigraphic sections of the units and component lithologies in the Ozark Region (left) and the Ouachita Mountains (right). Additionally shown are the stratigraphic locations of samples analyzed for this study (triangles) and previous studies [9,10], and the hosts of the Northern Arkansas and the Tri-State ores (black and blue bars, respectively). The height of the columns is not intended to represent the thicknesses of the units. Information on the units and lithologies is from: <https://www.geology.arkansas.gov/geology/stratigraphy.html> (accessed on 29 December 2020). Modified from [10].

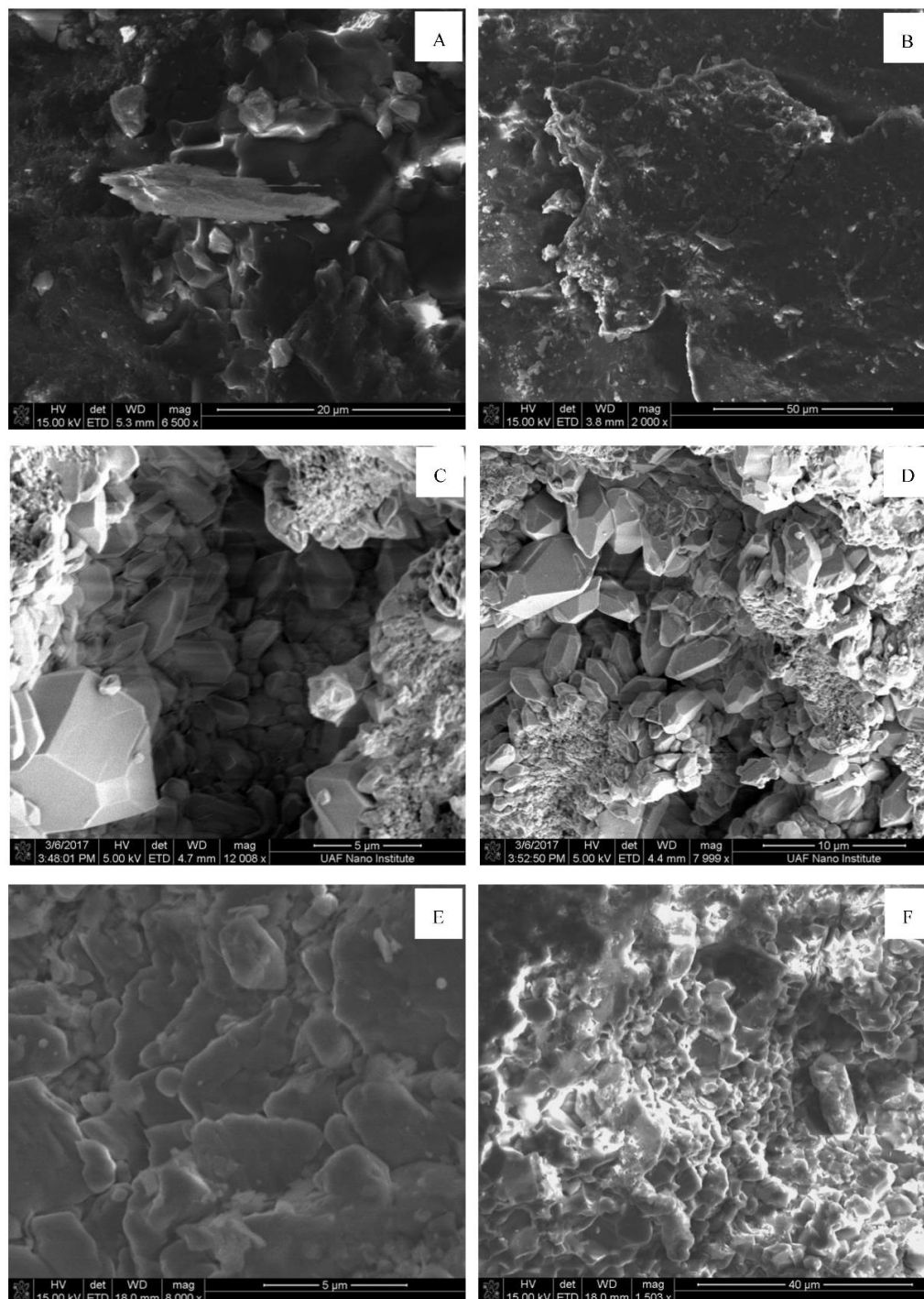


Figure 4. Scanning electron microscope secondary electron (SEM-SE) images of dolomite from the Cotter Dolomite (A,B), quartz from the tripolitic chert of the Boone Formation (C,D), and quartz from the Bigfork Chert (E,F).

Late diagenetic dolostones exhibit porosities and permeabilities significantly greater than those of early diagenetic replacement dolostones [37]. Late diagenetic dolomitization of the Knox was related to secondary porosity development, hydrocarbon migration, and local MVT mineralization [37]. In a similar way, dolomitization of the carbonate facies that host mineralization in the Upper Cambrian Bonneterre Dolomite in the Southeastern Missouri MVT district was of early diagenetic origin, and later underwent neomorphic recrystallization and cementation during exposure to mineralizing fluids [38–40]. Central and East Tennessee MVT ores, and part of Northern Arkansas MVT ores, are hosted

by the Cambro-Ordovician Knox and Early Ordovician Cotter dolomites, respectively. Hydrothermal dolomite cement commonly associated with trace amounts of sulfides results from hydrothermal alteration and dissolution followed by recrystallization through acid-producing reactions caused by fluid mixing within host carbonate rocks [41,42].

The carbonate sediments that make up the Lower Mississippian Boone Formation were produced on a broad, shallow carbonate platform, designated the Burlington Shelf [43]. The shelf occupied much of the central south-central midcontinent and rested on the Salem Plateaus. The lower Boone Formation reflects the Lower Mississippian maximum flooding interval on the Burlington Shelf [44]. In turn, the upper Boone Formation marks the highstand-regressive intervals and consists of sand to gravel size bioclastic grains [45].

The Boone Formation hosts three different types of chert. Penecontemporaneous chert is found within the lower Boone Formation as dark and nodular chert that formed within, and also as an early replacement of partially lithified carbonate sediment in a deep-water setting during maximum flooding conditions [13,46]. The highstand-regressive sequence recognized as the upper Boone Formation hosts two types of chert. The first type is grey to white, generated during a later diagenetic event. This diagenetic chert is a post-depositional replacement facilitated by the flow of groundwater along the bedding planes of the various, shallow water, carbonate lithologies [46,47]. This imparts an apparently interbedded chert and limestone character to the interval [48].

The upper Boone Formation also contains highly weathered, later diagenetic chert, located between the abovementioned diagenetic chert and underlying penecontemporaneous chert [14,47]. The key to producing the highly weathered chert is the initial presence of disseminated carbonate in the diagenetic chert [48,49]. This highly weathered diagenetic chert, named tripolitic chert [47,50], forms as a decalcitization of the included carbonate remaining in the later diagenetic chert [48]. The interval is 15–18 m thick, massive, white, and consists of highly leached diagenetic chert and lenses of unsilicified limestone [47,51,52]. The tripolitic chert experienced a second, silica-rich hydrothermal fluid flow, evidenced by the microscopic quartz druse present in voids produced by the earlier decalcitization [48,50] (Figure 4C,D). Leaching of fine-grained diagenetic chert of the upper Boone Formation by hydrothermal fluids is part of the tripolitic chert formation process that left significant dissolution channels along their interaction path. The hydrothermal events reflect lateral secretion produced by the Ouachita Orogeny beginning in the middle to late Pennsylvanian.

The renewed uplift of the Ozarks resulting from the Ouachita Orogeny exposed the region to faulting and fracturing, followed by broad and extensive weathering and erosion. All but a few outliers of the Pennsylvanian deposits have been removed from the Ozark Plateaus.

2.2. The Ouachita Mountains

The Ouachita fold-thrust belt was formed by the collision of the passive margin of Laurentia and an accretionary wedge forming on the front of a north-facing island arc [53]. The belt consisted of strata deposited in deep-water settings that underwent deformation by compressional events associated with plate collision along the southern border of what is now North America during Late Pennsylvanian and Permian time. The bulk of the belt is confined to the subsurface, with the only exposed portions located in central Arkansas, eastern Oklahoma, and the Marathon Uplift, west Texas [54]. The general structure of the Ouachita Mountains is a broad anticlinorium and synclinorium that experienced numerous thrust faults during the collision [55]. Late Cambrian to Early Ordovician strata are exposed in its center, while mostly Mississippian and Pennsylvanian strata are exposed along its margins [53]. Normal faulting against the Gulf Coastal Plain and Mississippi Embayment (Figure 2) led to infilling of this region to the east with a thick interval of sedimentary rocks, reaching a maximum thickness of about 5500 m [56].

The Middle-Late Ordovician Bigfork Chert (Figure 3; Figure 4E,F), one of the several, major siliceous units in the Ouachita Mountains, including the Arkansas Novaculite,

was deposited in a sediment-starved basin and consists of thinly bedded, dark gray, cryptocrystalline chert [57]. The chert is interbedded with various intervals of siliceous black shale, calcareous siltstone, and dense, bluish gray limestone [57,58]. Following its deposition in this basinal setting, the Bigfork Chert was folded and faulted in response to compressional forces associated with the Ouachita Orogeny.

The Mississippian Hatton Tuff was deposited near the bottom of the Stanley Shale in the Ouachita Mountains (Figure 3). It is massive, homogenous, and mostly devitrified, with inclusions of basalt, sandstone, slate, limestone, and fossils, predominately resembling a porphyritic igneous rock [59]. The unconformable contact between the base of the Stanley Shale and the “tripolitic” upper Arkansas Novaculite [58] in the Ouachita region has been stratigraphically shown to correlate with the contact between the lower and upper Boone Formation in the Ozark region (Figure 3). Unconformities often act as conduits with porous structure and permeability through fracturing, erosion, and further groundwater interaction. Thus, unique flow paths and capping aquitards in the Stanley Shale have produced a very likely system for the initial pulse of MVT brines in route to their final site of deposition.

2.3. The Mississippi Valley-Type Ore Deposits

Many MVT deposits were formed during Devonian to Permian time as a result of tectonic events reflecting amalgamation of Pangaea [1,16]. The Alleghenian-Ouachita Orogeny (Pennsylvanian–Permian) is responsible for the MVT mineralization in the Appalachian and the midcontinent regions (Figure 1). Dates for mineralization of what are now the Pb-Zn districts overlap with the waning stages of Appalachian and Ouachita tectonism. The ore deposits are often located where organic-rich shales onlap platform carbonate margins on the flanks of sedimentary basins [60] (Figure 1). Based on observations from southeastern Missouri and northeastern Arkansas, stylolites and fractures both acted as fluid-flow conduits throughout the subsurface. Mineralization accompanied deformation events, as recorded by these structures as evidence of directional fluid flow controls, in addition to intergranular flow through pore space [61]. Tectonic setting is not a first-order control on MVT ore-forming processes [62]. Topography-driven fluid flow is credited as the most robust fluid-drive mechanism for many MVT districts [4,16]. The tectonic uplift following the Late Pennsylvanian Alleghenian and Ouachita orogenic events created the topography necessary for driving brines out of the basins and into adjacent domes where the ores formed [4]. Ores along the Southeastern Missouri district may reflect a brine discharge pathway driven to the west out of the Appalachian foredeep and Illinois sag [4] (Figure 1). Later uplift in the southern Appalachians caused a northwest-oriented brine discharge out of the Black Warrior Basin into southeastern Missouri [4]. The Ouachita Orogeny facilitated the movement of MVT-forming hydrothermal fluids northward from the uplifted Arkoma foreland basin onto the Cambrian to Pennsylvanian carbonate platform of the Ozark Dome, where ores in the southern Ozark region are hosted [62] (Figure 1). The ore fluids have been shown to be mainly derived from evaporated seawater [42]. The Ouachita foreland experienced syn-collisional normal faulting, striking east–west and parallel to the orogen, which may have also helped facilitate the movement of hydrothermal fluids northward [63]. The epigenetic deposits occur principally in limestones and dolostones as open-space fillings, collapse breccias and as replacement of the carbonate host rock. The dominant ores are represented by sphalerite (ZnS) and galena (PbS), with minor amounts of iron sulfides, carbonates, barite, and fluorite forming typically as gangue minerals [42].

In the Tri-State district (1800 km²), six major deposits trending southwest–northeast are primarily hosted by cherty limestones of the Lower Mississippian Boone Formation (Figure 3) [64]. The ore deposition in this district is controlled by the Miami Fault [64]. One of the most productive mining fields in the world, the Picher Field encompasses about 350 km² and it was mined from the 1870s to the 1970s [65]. The field is overlain by a rather thin interval of nearly flat-lying Mississippian and Pennsylvanian strata. Based on Th-Pb dating of ore-stage calcite, the main-stage mineralization in the Tri-State district

has been constrained to the Late Permian—Early Triassic (251 ± 11 Ma) [66]. As of 1964, approximately 22,639,000 and 3,732,000 tons of zinc and lead concentrates respectively, had been produced from this large district [64]. At least 250 small ore bodies comprise the Northern Arkansas district, with ores hosted by rocks of Ordovician and Mississippian age (Figure 3): the Ordovician Cotter Dolomite, Powell Dolomite, and Everton Formation, and the Mississippian Boone Formation and Hindsville Limestone [67]. A common feature of the Northern Arkansas district is its proximal location to normal faults, which provided brine pathways that rose from deeper Cambrian-Ordovician carbonate aquifers into shallower sequences dominated by limestones [67]. Steeply dipping fractures and faults intersect breccias in karst-like system situated in close vicinity to ores [67]. Hence, breccias provided high porosity and high permeability, important for metal precipitation from advancing mineralizing fluids [68]. Similar to the Tri-State district, the rocks of the Northern Arkansas district are not highly deformed or structurally complex, with only minor local folding and a low regional dip to the south [67]. Paleomagnetic studies [69] provide strong constraints on the age of mineralization (Permian; 265 ± 20 Ma) in the Northern Arkansas district. Between 1907 and 1930, production figures for Zn and Pb were 29,000 tons and 1920 tons, respectively [67].

3. Materials and Methods

A total of 25 samples (Table S1 and Figure 2) were collected and analyzed for their trace element concentrations (REE, Pb, Th, and U) and Pb isotope ratios. Care was taken at the outcrop to collect as fresh and unaltered specimens as possible. A total of 5 samples of Lower Ordovician Cotter Dolomite (Figure 4A,B) were collected as large blocks from the Springfield-Salem Plateaus in southern Missouri and northern Arkansas. Overall, 13 tripolitic chert samples (Figure 4C,D) of the Mississippian Boone Formation were taken near the town sites of Pineville (MO), Lanagan (MO), and Bella Vista (AR). In total, 5 samples from the bedded Middle-Upper Ordovician Bigfork Chert (Figure 4E,F) were collected from the Ouachita Mountains in west-central Arkansas. The two samples from the Mississippian Hatton Tuff were collected from the Ouachita Mountains in western Arkansas.

Processing of the whole-rock samples was carried out in the rock room section of the class 100 Radiogenic Isotope Clean Laboratory at the University of Arkansas. The samples were sawed into approximately 1 cm thick slabs using a MK wet cutting tile saw. Following several cleaning steps, the slabs were powdered using a Spex SamplePrep Shatterbox and placed in acid-cleaned polypropylene specimen storage containers. The chemical processing of the rock samples was done in the modular section of the clean laboratory. For sample dissolution, 0.3 g of each powdered sample was placed in acid-cleaned PFA (perfluoroalkoxy alkanes) vials and processed through a series of high-purity heated acid attacks, including concentrated HF, 7 N HNO₃, and 6 N HCl. The chemical attacks allow complete digestion of the rock samples. The dissolved sample solution was dried down and 1 mL of concentrated HNO₃ was added to it. Following this step, the sample solution was placed on the hot plate set at 90° and dried down one more time. A subsequent addition of 2 mL 7 N HNO₃ to the sample was required to redissolve the sample. A volume of 0.2 mL of sample was removed and mixed with 4.8 mL of triple distilled water to obtain a sample solution in 2% HNO₃, ready to be analyzed for trace element concentrations.

For Pb isotope processing, the remainder 1.8 mL solution was dried down. In total, 2 mL 1 N HBr were added to each sample, allowed to re-dissolve, and dried down. This step was repeated two more times. The samples were then re-dissolved in 1 mL 1 N HBr and transferred in 1.5 mL acid-cleaned centrifuge tubes. Lead was separated and purified using cation exchange columns and an HBr medium. In preparation for column chemistry, around 150 µL resin (Dowex AG1-8X, 200–400 mesh) used to separate the Pb from any other ions was added to acid-cleaned syringes. For column conditioning, 2 mL 0.5 N HNO₃, 2 mL triple distilled water, and 2 mL 6 N HCl were successively added to the columns and allowed to drip through.

The samples, dissolved in 1 mL 1 N HBr, were then transferred from the centrifuge tubes to the columns and allowed to drip through. Before sample collection, each sample was rinsed in three successive additions of 1 mL 1 N HBr. For sample collection, 1 mL 20% HNO₃ was added and collected in clean Teflon containers, and then placed on a hot plate to dry. The samples were subsequently diluted with 2% HNO₃ containing 4 ppb Tl just before the isotopic analysis.

For trace-element concentration analysis, 25 samples, one duplicate (LT 1D), and one blank were processed. The trace element concentrations were analyzed on a Thermo Scientific iCAP Q ICP-MS, located in the Trace Element and Radiogenic Isotope Laboratory at the University of Arkansas. To avoid polyatomic interferences, a kinetic energy discrimination (KED) collision cell was used. This cell provides a clearer ICP-MS spectra and better detection power for interfering isotopes. A high purity U.S. Geological Survey multi-element standard diluted to various concentrations (1, 5, 10, 50, and 100 ppb) was measured along with the samples to build calibration curves and constrain the accuracy and reproducibility of the measurements. Analytical precision for La and Ce was better than 2% relative standard deviation (RSD); for Sm, Tm, and Th, the precision was 3% (RSD) or better; for Nd, Eu, Tb, Dy, Er, Yb, Lu, Pb, and U, the precision was 4% (RSD) or better; for Pr and Gd, and Ho, the precision was 5% (RSD) or better. Replicate analyses indicate that measurement reproducibility for all REE was 4% or better. Data normalization was conducted for each sample by reducing recorded intensities to concentrations based on the aforementioned standard. One blank for the water and the acids used in sample processing was run throughout the analyses, accounting for negligible external contamination. The results of the trace element concentration analyses are found in Table S2.

Lead isotope analyses of whole rocks were carried out on a Nu Plasma multi-collector ICP-MS located in the Trace Element and Radiogenic Isotope Laboratory at the University of Arkansas using a DSN 100 desolvating system. The Pb-Tl mixtures were normalized using the Tl normalization technique for mass bias correction [70]. The data collected for each sample represent averages of 60 ratios per sample. Analyses of the NBS 981 Pb standard carried out during the analyses (October 2018 and May 2019) produced the following results $^{208}\text{Pb}/^{204}\text{Pb} = 36.6576 (\pm 7.75 \times 10^{-5} 1\sigma)$; $^{207}\text{Pb}/^{204}\text{Pb} = 15.4796 (\pm 2.33 \times 10^{-5} 1\sigma)$; $^{206}\text{Pb}/^{204}\text{Pb} = 16.9230 (\pm 7.75 \times 10^{-5} 1\sigma)$. All standard and sample Pb data were normalized to $^{205}\text{Tl}/^{203}\text{Tl} = 2.38750$, and raw data were corrected using the sample-standard bracketing method and accepted values for the Pb standard ($^{208}\text{Pb}/^{204}\text{Pb} = 36.7006$; $^{207}\text{Pb}/^{204}\text{Pb} = 15.4891$; $^{206}\text{Pb}/^{204}\text{Pb} = 16.9356$) [71]. Lead blank levels for both the water and acids used in sample processing were uniformly better than 4 pg/g. The measured Pb isotope compositions of the analyzed rocks have been age corrected for in situ U and Th decay to 250 Ma (Table S3), the approximate age of mineralization [66,69].

4. Results

4.1. Rare Earth Element (REE) Patterns

The REE concentration patterns produced by the analyzed samples are illustrated by REE diagrams (Figure 5A), which display REE depletion (negative inflections) or REE enrichment (positive inflections) relative to those of the North American Shale Composite (NASC) [72]. Normalization removes any natural variations in absolute REE concentrations of REE, allowing comparison with the REE of the upper crust, for which shale is a proxy [24]. The REE_{SN} (NASC-normalized REE) values for all samples are less than 1, with the lowest normalized REE values found in the Cotter Dolomite.

The REE patterns (Figure 5A) for the majority of the tripolitic chert sampled from the Boone Formation exhibit a relatively flat shale-normalized distribution pattern. Only two of the five Bigfork Chert samples show moderate enrichment in the LREE (light REE) relative to the HREE (heavy REE), while all Cotter Dolomite samples are enriched in the LREE relative to the HREE. A different trend is shown by the Hatton Tuff samples, with moderate enrichment in the HREE relative to the LREE.

Each tripolitic chert sample has a low abundance of Ce compared to their neighboring REE, and only one of the five Cotter Dolomite samples has a very low Ce abundance compared to the neighboring REE. The Ce_{SN}/Ce^*_{SN} ratio is the simplest approach to quantify the redox-related decoupling of Ce from the other REE, which produces Ce anomalies in the REE_{SN} patterns [73], where $Ce_{SN}/Ce^*_{SN} = Ce_{SN}/(0.5*La_{SN} + 0.5*Pr_{SN})$. The majority of the analyzed samples show small to moderate negative Ce anomalies. The Ce_{SN}/Ce^*_{SN} ratios of the Cotter Dolomite range between 0.87 and 0.94, with one anomalously low value of 0.05, those of the Bigfork Chert vary between 0.77 and 0.99, and those of the tripolitic chert range between 0.31 and 0.79. The two Hatton Tuff samples display small positive Ce anomalies (1.28 and 1.45; Table S2).

Except for Ce, Eu is the only REE for which anomalies due to redox reactions are seen in aqueous solutions and their precipitates [74]. The majority of the analyzed samples have small to moderate negative Eu anomalies, as indicated by Eu_{SN}/Eu^*_{SN} ratios of less than 1 (Table S2), where $Eu_{SN}/Eu^*_{SN} = Eu_{SN}/(0.5*Sm_{SN} + 0.5*Gd_{SN})$. Only two Cotter Dolomite samples have small positive Eu anomalies (1.03 and 1.47). Eu_{SN}/Eu^*_{SN} ratios that have been determined for the Bigfork Chert samples range between 0.72 and 0.91, those for the tripolitic chert of the Boone Formation vary between 0.83 and 0.94, for the Cotter Dolomite between 0.79 and 1.47, and for the Hatton Tuff between 0.45 and 0.48.

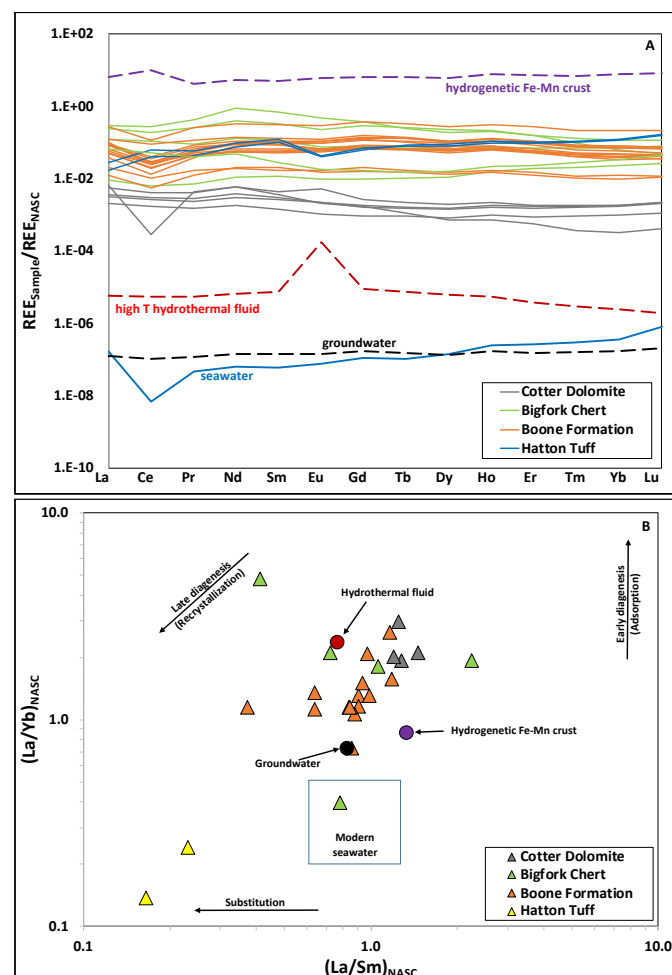


Figure 5. (A) North American Shale Composite (NASC)-normalized [72] REE distribution patterns in the analyzed samples. Additionally shown are values for seawater [75,76], groundwater from Ash Meadows, Nevada [26], high temperature hydrothermal fluid from the Broken Spur site at the Mid-Atlantic Ridge [77], and hydrogenetic Fe-Mn crust [78]. (B) $(La/Sm)_N$ vs. $(La/Yb)_N$ plot displaying the $(La/Sm)_N$ values vs. the LREE-HREE fractionation proxy in the analyzed samples.

On a $(\text{La}/\text{Sm})_{\text{SN}}$ vs. $(\text{La}/\text{Yb})_{\text{SN}}$ plot, the majority of the samples have $(\text{La}/\text{Sm})_{\text{SN}}$ ratios within the modern seawater range (0.60 to 1.60; [79]) (Figure 5B). However, the values of the $(\text{La}/\text{Yb})_{\text{SN}}$ proxy are higher, suggesting that diagenetic processes affected the samples to a variable extent. Overall, the oldest samples, which are Cotter Dolomite, exhibit the highest LREE-HREE fractionation among all analyzed samples and have $(\text{La}/\text{Sm})_{\text{SN}}$ values slightly higher compared to modern seawater (Figure 5B).

4.2. Lead Isotope Signatures

The Pb isotope ratios of the analyzed samples are reported in Table S3. Figure 6 represents covariate diagrams displaying the measured (A,B) and age-corrected (C,D) Pb isotope ratios of the samples. All present day Pb isotope values were age corrected to 250 million years corresponding to the formation of the ores, allowing comparison with the ore deposits and evaluation of the potential genetic relationship between the analyzed samples and the ores. However, it is important to recognize that the U-Th/Pb ratios may have changed in these multiply altered rocks for 250 Ma. The Pb, Th, and U concentrations used for age corrections are found in Table S2.

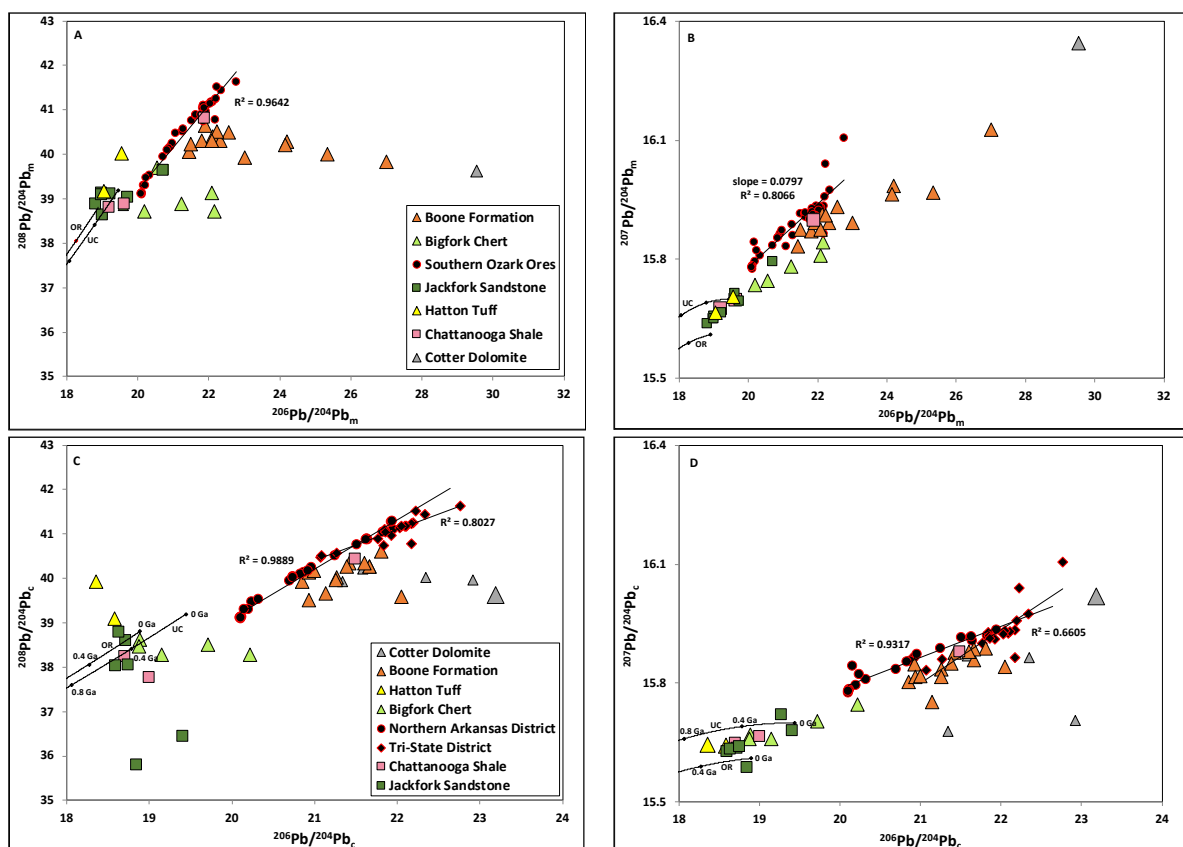


Figure 6. Measured (A,B) and age-corrected (C,D) Pb isotope ratios of analyzed samples. Additionally shown are published results of Chattanooga Shale [9], Jackfork Sandstone [10], and MVT ores from the Northern Arkansas and the Tri-State mining districts [9,28,80]. Linear trends through the MVT ores from the southern Ozark region (A,B), Northern Arkansas (C,D), and Tri-State (C,D) are also displayed. The average orogene (OR) and upper crust (UC) growth curves are included [81]. In total, four of the Cotter Dolomite samples with μ ($^{238}\text{U}/^{204}\text{Pb}$) values over 200 have been omitted from the measured Pb isotope plots (A,B) and represented with smaller symbols on the age-corrected Pb isotope plots (C,D).

Overall, the tripolitic chert samples of the Boone Formation have lower measured $^{208}\text{Pb}/^{204}\text{Pb}$ and $^{207}\text{Pb}/^{204}\text{Pb}$ values for a given $^{206}\text{Pb}/^{204}\text{Pb}$ compared to the MVT ores (Figure 6A,B). Except for the Hatton Tuff, all analyzed samples plot to the right of both growth curves, with the Cotter Dolomite samples displaying the highest $^{207}\text{Pb}/^{204}\text{Pb}$ and

$^{206}\text{Pb}/^{204}\text{Pb}$ ratios. The Bigfork Chert samples have lower $^{208}\text{Pb}/^{204}\text{Pb}$ and $^{207}\text{Pb}/^{204}\text{Pb}$ for a given $^{206}\text{Pb}/^{204}\text{Pb}$ compared to the Boone Formation (Figure 6A,B). Fitted regression lines through the southern Ozark ores on the thorogenic (Figure 6A) and uranogenic (Figure 6B) diagrams yield coefficients of determination of 0.9642 and 0.8066, respectively.

Age-corrected Pb isotope ratios of several tripolitic chert overlap, on both isotope plots, with those of ores from the Northern Arkansas district, which are collinear with and less radiogenic than the Tri-State ores (Figure 6C,D). The Cotter Dolomite samples show lower $^{208}\text{Pb}/^{204}\text{Pb}$ and $^{207}\text{Pb}/^{204}\text{Pb}$ for a given $^{206}\text{Pb}/^{204}\text{Pb}$ compared to the MVT ores. Overall, the Cotter Dolomites display a wider range of $^{206}\text{Pb}/^{204}\text{Pb}$ ratios compared to all analyzed samples. In total, two Bigfork Chert samples plot close to the 0.4 Ga upper crust reservoir and three Bigfork Chert samples plot below the same reservoir (Figure 6C). Another two Hatton Tuff samples plot to the left of the orogene curve, showing ^{208}Pb -enriched signatures.

On the uranogenic diagram (Figure 6D), the majority of the tripolitic chert samples are collinear with and less radiogenic than ores from the Tri-State district. The Cotter Dolomites display a wide range of $^{207}\text{Pb}/^{204}\text{Pb}$ and $^{206}\text{Pb}/^{204}\text{Pb}$ values relative to other analyzed samples. Overall, the dolomites are radiogenic in comparison to the recorded values of other formations in this study. The Hatton Tuff samples and three of the Bigfork Chert samples plot between the upper crust and the orogene growth curves, while two Bigfork Chert samples plot to the right of the upper crust growth curve (Figure 6D).

5. Discussion

5.1. Diagenetic History of Sampled Formations

Rare earth elements are supplied to the world's oceans through rivers, aeolian input, and hydrothermal vents, and are removed during sedimentation via particle scavenging [24]. The relative concentrations of REE in rivers resemble those of cratonic shales and greatly influence the chemistry of continental shelf waters [82]. The rapid transport into the deep ocean of the REE scavenged by the surface ocean and their release from the sediment explains the similar REE patterns found in deep and surface waters [25]. Rare earth elements are highly enriched in carbonates (ppm) formed diagenetically compared to natural fluids, such as seawater, river water, and groundwater (10^{-6} to 10^{-3} ppm) [27,83,84]. Carbonates precipitated by living marine organisms have low abundances of REE (parts per billion), while similar carbonates in seafloor sediments have much higher abundances (1–2000 ppm) [85–87]. The enrichment of REE in the latter carbonates occurs during the interaction of sediment with pore and bottom waters near the sediment–water interface [27,85,86].

The typical seawater REE profile (Figure 5A) shows progressive enrichments in heavier REE relative to lighter REE [24]. Deviations from this trend occur when an element in the REE series has a unique property that affects its solubility and removal via scavenging onto Fe–Mn (oxyhydr)oxides, organic matter, and clay particles [24]. This results in positive La, Eu, Gd, and Lu anomalies, and negative Ce anomalies in seawater. Larger, positive Eu anomalies may indicate mixing of seawater with hydrothermal fluids [88]. The sampled lithologies for this study do not yield the features that are typical of REE distribution of modern seawater (Figure 5A). The lack of preservation of characteristic seawater anomalies in the REE distribution pattern in authigenic minerals implies that the sample, deposited initially in marine conditions, has been secondarily altered [24]. This is also shown by the values of the $(\text{La}/\text{Yb})_{\text{SN}}$ proxy (Figure 5B), which indicate LREE–HREE fractionation and suggest that diagenetic processes affected the samples to a variable extent.

Cerium and Eu are the only REE for which anomalies due to redox reactions are seen in aqueous solutions and their precipitates [74]. The Ce anomaly results from oxidation of Ce^{3+} to Ce^{4+} and subsequent decoupling of Ce from the other REE in response to formation of the less soluble Ce^{4+} species, which are preferentially adsorbed on particle surfaces [74]. This results in a pronounced negative Ce_{SN} anomaly in recent seawater, which is mirrored by a strong positive anomaly in recent ferromanganese nodules and crusts [25]. Most commonly, Ce anomalies are used as a proxy to identify oxygenation of

the marine environment during the Precambrian, or Phanerozoic anoxic events ([24] and references therein). Cerium anomalies are more pronounced in the Mississippian tripolitic chert samples (0.31–0.58) for this study, while the lower Ordovician Cotter Dolomite shows minimal Ce anomalies (0.87–0.94). This low Ce anomaly in the Cotter Dolomite may reflect the influences of detrital components during diagenesis and incorporation of mobilized REE from local detrital phases into diagenetic carbonates. However, the low Ce anomaly may also indicate anoxic marine conditions during deposition. The first possibility is supported by the high LREE-HREE fractionation (Figure 5B), generally the highest among the studied formations.

The negative Ce anomalies shown by all tripolitic chert sampled for this study (Figure 5A) signal a well-oxygenated depositional environment. On a $(La/Sm)_{SN}$ vs. $(La/Yb)_{SN}$ plot, one tripolitic chert sample and groundwater overlap (Figure 5B), suggesting possible interaction of groundwater with the Boone Formation. Therefore, current geochemical data support interpretations by previous studies that diagenetic cherts are a post-depositional replacement facilitated by the flow of groundwater along the bedding planes of the various, shallow water, lithified carbonate lithologies [46,47]. Moreover, the value of the $(La/Yb)_{SN}$ proxy for several tripolitic chert samples resembles that of hydrothermal fluids (Figure 5B), supporting previous studies that tripolitic chert also experienced hydrothermal fluid flow, evidenced by the microscopic quartz druse present in voids produced by the earlier decalcitization [48,50].

Decoupling of Eu from the other REE under diagenetic conditions has been reported in previous studies [89] and attributed to preferential Eu mobility due to reduction in Eu^{3+} . However, formation of significant quantities of Eu^{2+} is restricted to extremely reducing conditions and elevated temperatures [90]. Eu^{3+} is perhaps the dominant valence occurring under most diagenetic conditions [90]; therefore, negative Eu anomalies in seawater and marine sediments may reflect the crustal source of the REE [25]. The average Eu_{SN}/Eu^*_{SN} ratio for the upper crust is 0.65 ± 0.05 [91], indicating that most analyzed samples were subject to lower degrees of Eu fractionation compared to the upper crust. However, there are two exceptions to this relationship, represented by two Cotter Dolomite and two Hatton Tuff samples collected for this project. Pronounced positive Eu_{SN} anomalies and enrichment of the LREE over the HREE are both patterns characteristic of high-temperature hydrothermal fluids [77]. Higher Eu_{SN}/Eu^*_{SN} values in two Cotter Dolomites (1.031 and 1.473) suggest involvement of high-temperature solutions or detrital components. This is also supported by the $(La/Yb)_{SN}$ values of the Cotter Dolomite samples, which are similar to those of hydrothermal fluids (Figure 5B). Both REE and isotopic studies of the regionally extensive dolomites from the Mississippian Burlington-Keokuk Formation concluded that there were two major generations of dolomite production, formed in distinctly different diagenetic environments [25]. The first generation inherited its REE from Mississippian seawater or marine pore-waters. The second generation was formed by the subsequent recrystallization of that first generation produced by non-marine diagenetic fluids [20]. Based on the geochemical data presented herein, it appears that the Cotter Dolomite might have experienced a diagenetic history similar to that of the second generation of dolomites within the Mississippian Burlington-Keokuk Formation.

The Hatton Tuff samples, collected at the base of the Mississippian Stanley Shale, in the Ouachita Mountain region, produced the most pronounced negative Eu_{SN} anomalies (0.451 and 0.484) of all sampled lithologies and, unlike all other analyzed samples, have pronounced positive Ce_{SN} anomalies (1.453 and 1.276) (Table S2). The tuff samples also have the lowest $(La/Yb)_{SN}$ and $(La/Yb)_{SN}$ values (0.240–0.137 and 0.230–0.165, respectively) of all samples (Figure 5B). As expected, this suggests a different origin and evolution compared to all other samples. Studies of paleocurrent, grain size distribution, and geometry of the Hatton Tuff also suggest a volcanic source to the south and southeast [92].

The $(La/Yb)_{SN}$ values of three upper Ordovician Bigfork Chert samples are similar to those of hydrothermal fluids, suggesting the influence of these fluids on the chert (Figure 5B). The samples show less pronounced negative Ce anomalies and generally

higher LREE-HREE fractionation compared to the tripolitic chert of the Boone Formation. Relative REE abundances, Ce and Eu anomalies, and the $(La/Yb)_{SN}$ proxy suggest that the Cotter Dolomite was subject to an increased degree of alteration compared to the Bigfork Chert and chert from the Boone Formation.

5.2. Constraints on the Potential Source of Ore Metals

The age corrected Pb isotope ratios for the tripolite and the Cotter Dolomite samples display characteristics typical of “J-type” Pb, similar to the ore samples. “J-type” Pb, named after their discovery site in Joplin, MO [93], are enriched in radiogenic Pb isotopes relative to common Pb. The Pb isotope ratios of this anomalous Pb do not fit the single-stage model of Pb evolution (Holmes–Houtermans model of common Pb, 1946) and require interpretation by the two-stage model (Stacey and Kramers model, 1975). The two-stage growth curve approximates the orogene growth curve [81]. On the thorogenic and uranium diagrams (Figure 6), age corrected Pb isotope ratios for the tripolitic chert and the Cotter Dolomite samples plot far to the right of the 0 Ga upper crust and orogene Pb reservoirs of [81].

Available Pb isotope values of ores from the Northern Arkansas and Tri-State districts are enriched in radiogenic Pb (Figure 6). The ores display a range of Pb isotope ratios that form linear trends, but are better defined in case of the Northern Arkansas ores. On the thorogenic (Figure 6C) and uranium (Figure 6D) diagrams, fitted regression lines through the Northern Arkansas ores yield coefficients of determination of 0.9889 and 0.9317, respectively. However, same regression lines through the Tri-State ores (Figure 6C,D) yield lower coefficients of determination of 0.8027 and 0.6605, respectively. The linear trends are conventionally, however not always, interpreted to result from the mixing of two end-member components or from a single source of Pb that contains variable Pb isotope compositions [15]. In case of mixing, one end-member must be highly radiogenic, with Pb isotope ratios higher than the highest value for ores. The other end-member must be less radiogenic, with Pb isotope ratios equal to or lower than the lowest value recorded for ores. Generally, the enriched Pb isotope compositions have been interpreted to represent a crustal source likely resulting from heated basinal brines flowing through paleo-aquifers [36,94]. Hydrothermal fluids generated as a result of the Ouachita Orogeny interacted with Precambrian basement and Paleozoic carbonate and clastic formations as they moved northward to the depositional sites of the MVT ore deposits. Precambrian basement as well as carbonate cements in Paleozoic sandstone aquifers have been recognized as possible sources of Pb [6,8]. Other studies have indicated that Pb was supplied by two end-member components and have suggested that the best candidates for contributing the less radiogenic end-member to the ores were the shales of the lowermost section of the Chattanooga Shale (Devonian) [9] or the sandstone members of the upper and middle Jackfork Sandstone (lower Pennsylvanian) [10] (Figures 2, 3 and 6).

The low Pb concentrations in the tripolitic chert of the Boone Formation and the Cotter Dolomites analyzed in this study, in most cases less than 1 ppm (Table S2), would preclude them from representing a major source of ore Pb today. However, the ore forming process in the southern Ozark region occurred approximately 100 Ma after deposition of the Boone Formation and more than 200 Ma after deposition of the Cotter Dolomite. The REE studies presented in the previous section demonstrated that diagenetic processes affected the samples to a variable extent. Therefore, it is highly possible that, at the time of deposition, the analyzed rocks had high U/Pb and Th/Pb ratios and could therefore develop radiogenic Pb over time. The low present-day Pb concentrations in these rocks may partly be due to Pb removal by hydrothermal alteration. Under medium temperature conditions, like those encountered in hydrothermal environments, Pb is soluble [15]. However, another possibility that cannot be ruled out is that the hydrothermal fluids responsible for mineralization contributed ore Pb to the dolomites and to the tripolitic chert samples as they moved north through the Ozark Dome toward the emplacement of the Tri-State and the Northern Arkansas MVT ores.

The tripolitic cherts and the dolomites contain highly radiogenic Pb, with isotopic ratios comparable to those of the MVT ores in the southern Ozark region. However, the majority of analyzed rocks have lower $^{208}\text{Pb}/^{204}\text{Pb}$ and $^{207}\text{Pb}/^{204}\text{Pb}$ for a given $^{206}\text{Pb}/^{204}\text{Pb}$ compared to the MVT ores. Only one analysis from the Cotter Dolomite might qualify as a high-end component in $^{207}\text{Pb}/^{204}\text{Pb}$ vs. $^{206}\text{Pb}/^{204}\text{Pb}$ space, however the unit as a whole does not. Therefore, it appears that mixing is not a viable interpretation for the high-end component of the ore array based on the data available thus far. It is important to reiterate that some of the Northern Arkansas ores are hosted by the (Lower Mississippian) Boone Formation and the (Lower Ordovician) Cotter Dolomite, while the majority of the Tri-State ores are hosted by the Boone Formation.

The slope of the linear trend defined by the Pb isotope ratios of the southern Ozark region ores is 0.0797 (Figure 6B), which corresponds to an age of about 1.19 Ga. This implies input of Pb from a Precambrian source. Therefore, an alternative for the linear array is that the basement rocks supplied some ore Pb. In which case, the observed linear array in the Northern Arkansas ores represents a “pseudo-isochron” inherited, but not entirely, from the local basement. The Spavinaw Granite (1.40–1.35 Ga), which represents the Middle Proterozoic basement [95,96] underlying parts of Kansas, Oklahoma, Missouri, and Arkansas, is part of the Southern Granite-Rhyolite Province. Notably, the Southeast Missouri district, located to the E-NE of the study area, is underlain by the basement rocks of the St. Francois Mountains (1.42–1.48 Ga), which are part of the Eastern Granite-Rhyolite Province [8,95]. These two provinces cover a large part of the mid-continent US.

5.3. MVT Mineralization

The two common mechanisms by which many MVT deposits form is topography-driven fluid flow and density-driven groundwater and brine fluid flow [1–4]. The Appalachian and Ouachita orogenic events have created a hydraulic head through topographic relief in the Late Pennsylvanian to Early Permian that influenced the flow of hot brines north and northwest to form the Appalachian and mid-continent MVT deposits [1]. Fluids were expelled from the Arkoma Basin, the Black Warrior Basin, and the Appalachian Basin (Figure 1) into structurally controlled hydrologic domains [97]. Other potential mineralizing fluid contributors may be found in large sedimentary basins northwest and northeast of the Ozark Uplift (Figure 1), the Forest City Basin, and the Illinois Basin [68]. A lack of temporal overlap between gangue and metal sulfide deposition indicates that different fluid contributions to gangue and sulfide mineral deposition is possible and likely [98]. In the Dobson mine of the Tri-State MVT district, the sparse barite formed later than marcasite and earlier than the botryoidal calcite with which it is associated [65]. This indicates different periods of mineral formation, likely resulting from multiple pulses of hydrothermal fluids within the MVT deposits.

Most of the fluids originate from evaporated seawater or water that contains dissolved halite and has interacted with sedimentary rocks and, possibly, basement rocks [99]. The presence of an evaporitic environment in the hydrothermal fluid flow path appears to be necessary for the high salinities required for metal solubility and transport. Upper limits on possible metal concentrations in hydrothermal fluids are of similar magnitude to the highest measured concentrations of Pb, Zn, Cu, and Ba found in typical sedimentary brines [42]. As an example, in the region of the Paran fault in the Dead Sea area of Israel, it has been suggested that mixing of two metalliferous fluids led to dolomitization and mineralization [100]. The first of these fluids, with temperatures reaching 75 °C, is represented by the Mg-rich Dead Sea rift brine migrating deep in the subsurface prior to dolomitizing the carbonate bedrock. The highly soluble minerals typical of evaporite sedimentary rocks (halite, sylvite, gypsum, kieserite) precipitate from concentrated salt solutions or brines. Dissolution of such minerals is a source of dissolved chloride ions and sulfate. Thus, the brine supplies the chloride ions, which are important ligands that carry the metals in solution as chloride complexes prior to reaching their depositional environments. The second fluid, migrating at lower temperatures ($T \leq 50$ °C), is represented by the shallower

groundwater that acquired high solute concentrations from leaching igneous rocks and clastic sediments in the subsurface [100].

Hydrothermal fluids may interact with cooler oxygen-rich and oxidized meteoric waters, which may induce specific reactions such as H₂S oxidation as well as mixing and cooling corrosion. Further, solution aggressiveness can also be renewed or enhanced by mixing of waters with contrasting chemistry, particularly those differing in CO₂ and H₂S content or salinity. In addition, the conversion of H₂S to H₂SO₄ produces a sharp increase in dissolution as sulfuric waters become more aggressive with production of sulfuric acid [101]. In the southern Ozark region, faults near Lanagan and Pineville, Missouri (Figure 2) may have produced a number of pathways for the hydrothermal fluids from the east/southeast. To the north and east, MVT brine fluids may have also interacted with meteoric or connate waters of the Ozark Plateaus aquifer system, represented by the St. Francois aquifer (Cambrian), the Ozark aquifer (Ordovician), and overlying Springfield Plateau aquifer (Mississippian). The Cotter Dolomite and the tripolitic chert of the upper Boone Formation are part of the Ozark and the Springfield Plateau aquifers, respectively. Previous studies [8] suggested geologic units of the St. Francois aquifer (Lamotte Sandstone and Bonneterre Dolomite) could have been potential ore metal sources for the Southeast Missouri Lead Belts.

The hydrothermal fluid that produced the tripolitic chert within the Mississippian upper Boone appears to be similar to the second fluid in the Paran fault region. The porous texture of the tripolitic chert is the result of decalcitization of the carbonate remaining in the later diagenetic chert by interaction with meteoric or connate waters [48]. Quartz druse within the micro-porosity of the tripolitic chert suggests the presence of a second hydrothermal fluid pulse through the previously dissolved basal upper Boone Formation [48,50–52]. This second pulse of silica-rich hydrothermal fluid, reflecting lateral secretion produced by the Ouachita Orogeny in the middle to late Pennsylvanian, would have been confined by the penecontemporaneous chert of the lower Boone Formation below and the later diagenetic chert of the upper Boone Formation above [14]. This second pulse may also be responsible for generation of MVT ores.

6. Conclusions

The southern Ozark MVT ores display a range of Pb isotope ratios which form linear trends. On thorogenic and uranium diagrams, fitted regression lines through the Northern Arkansas ore distributions yield better coefficients of determination (0.9889 and 0.9317) compared to those of the Tri-State ores (0.8027 and 0.6605). The linear trends are usually interpreted to result from the mixing of two end-member components or from a single source of Pb that contains variable Pb isotope compositions. Precambrian basement, as well as carbonate cements in Paleozoic sandstone aquifers, have been recognized as possible sources of Pb [6,8]. Other studies have indicated that Pb was supplied by two end-member components and have suggested that the best candidates for contributing the less radiogenic end-member to the ores could have been the shales of the lowermost section of the Chattanooga Shale (Devonian) [9] or the sandstone members of the upper and middle Jackfork Sandstone (lower Pennsylvanian) [10]. Of remaining interest is identifying the source rock(s) that contributed the more radiogenic Pb to the MVT ores.

The tripolitic cherts of the Boone Formation and the Cotter Dolomite contain highly radiogenic Pb, with isotopic ratios comparable to those of the MVT ores in the southern Ozark region. However, the majority of the sampled lithologies have lower ²⁰⁸Pb/²⁰⁴Pb and ²⁰⁷Pb/²⁰⁴Pb for a given ²⁰⁶Pb/²⁰⁴Pb compared to the MVT ores. Therefore, it appears that mixing is not a viable interpretation for the high-end component of the ore array based on the data presented, suggesting that the source of the high Pb isotopic ratios may lay further afield. The slope of the linear trend defined by the Pb isotope ratios of the southern Ozark region ores corresponds to an age of about 1.19 Ga. Therefore, an alternative for the linear array requires involvement of the Precambrian basement with supplying ore Pb. The Spavinaw Granite (1.40–1.35 Ga), which represents the Middle Proterozoic basement [95,96]

underlying parts of Kansas, Oklahoma, Missouri, and Arkansas, is part of the Southern Granite-Rhyolite Province.

The sampled lithologies for this study do not yield the features that are typical for the REE distribution of modern seawater. The lack of preservation of characteristic seawater anomalies in the REE distribution pattern in authigenic minerals implies that those samples, deposited initially in marine conditions, have been secondarily altered [24]. This is also shown by the values of the $(La/Yb)_{SN}$ proxy, which indicate LREE-HREE fractionation and suggest that diagenetic processes affected the samples to a variable extent. Relative REE abundances, Ce and Eu anomalies, and the $(La/Yb)_{SN}$ proxy suggest that the Cotter Dolomite was subject to an increased degree of alteration compared to that of the Bigfork Chert and the Boone Formation. Based on the geochemical data presented, it appears that the Cotter Dolomite might have experienced a diagenetic history similar to that of the second generation of dolomites within the Mississippian Burlington-Keokuk Formation. Current data suggest a different origin and evolution of the Hatton Tuff compared to all sampled lithologies. Studies of paleocurrent, grain size distribution, and geometry of the Hatton Tuff suggest a volcanic source to the south and southeast [92].

Supplementary Materials: The following are available online at <https://www.mdpi.com/article/10.3390/geosciences11040172/s1>, Table S1: Type, age, and location of analyzed samples; Table S2: Rare Earth Elements, Pb, Th, and U concentrations in analyzed samples (in ppm); Table S3: Measured (m) and age-corrected (c) lead isotope ratios of analyzed samples.

Author Contributions: All authors contributed to the study conception and design. Material preparation, data collection and analysis were performed by J.C., S.E.M. and J.R.S. The final draft of the manuscript was written by J.C., with significant input from S.E.M. Revisions to the first draft were provided by A.P. and W.L.M. All authors have read and agreed to the published version of the manuscript.

Funding: This research received no external funding.

Institutional Review Board Statement: Not applicable for studies not involving humans or animals.

Informed Consent Statement: Not applicable for studies not involving humans.

Data Availability Statement: Data are contained within the article.

Acknowledgments: This study is possible thanks to the support of Erik Pollock and Barry Shaulis of University of Arkansas's Stable Isotope Laboratory and Trace Element and Radiogenic Isotope Laboratory, who assisted the authors in ensuring that the Nu Plasma ICP-MS and iCAP ICP-MS were functioning properly so that high-resolution Pb isotope and concentration data could be collected. The authors would also like to thank Mourad Benamara of Arkansas Nano and Bio Materials Characterization Facility for his help with acquiring the scanning electron microprobe images. The authors are grateful to the *Geosciences* journal reviewers for improving the manuscript through their insightful comments and critical reviews.

Conflicts of Interest: The authors declare no conflict of interest.

References

1. Leach, D.L.; Rowan, E.L. Genetic link between Ouachita foldbelt tectonism and the Mississippi Valley-type lead-zinc deposits of the Ozarks. *Geology* **1986**, *14*, 931–935. [[CrossRef](#)]
2. Appold, M.S.; Garven, G. The hydrology of ore formation in the Southeast Missouri district: Numerical models of topography-driven fluid flow during the Ouachita orogeny. *Econ. Geol. Bull. Soc. Econ. Geol.* **1999**, *94*, 913–936. [[CrossRef](#)]
3. Appold, M.S.; Nunn, J.A. Hydrology of the western Arkoma Basin and Ozark Platform during the Ouachita orogeny: Implications for Mississippi Valley-type ore formation in the Tri-State Zn-Pb district. *Geofluids* **2005**, *5*, 308–325. [[CrossRef](#)]
4. Garven, G.; Ge, S.; Person, M.A.; Sverjensky, D.A. Genesis of stratabound ore deposits in the midcontinent basins of North America: 1. The role of regional groundwater flow. *Am. J. Sci.* **1993**, *293*, 497–568. [[CrossRef](#)]
5. Doe, B.R.; Delevaux, M.H. Source of lead in southeast Missouri galena ores. *Econ. Geol. Bull. Soc. Econ. Geol.* **1972**, *67*, 409–425. [[CrossRef](#)]
6. Heyl, A.V.; Landis, G.P.; Zartman, R.E. Isotopic Evidence for the Origin of Mississippi Valley-Type Mineral Deposits: A Review. *Econ. Geol. Bull. Soc. Econ. Geol.* **1974**, *69*, 992–1006. [[CrossRef](#)]

7. Crocetti, C.A.; Holland, H.D.; McKenna, L.W. Isotopic composition of lead in galenas from the Viburnum Trend, Missouri. *Econ. Geol. Bull. Soc. Econ. Geol.* **1988**, *83*, 355–376. [[CrossRef](#)]
8. Goldhaber, M.B.; Church, S.E.; Doe, B.R.; Aleinikoff, J.N.; Brannon, J.C.; Podosek, F.A.; Mosier, E.L.; Taylor, C.D.; Gent, C.A. Lead and sulfur isotope investigation of Paleozoic sedimentary rocks from the southern Midcontinent of the United States; implications for paleohydrology and ore genesis of the Southeast Missouri lead belts. *Econ. Geol. Bull. Soc. Econ. Geol.* **1995**, *90*, 1875–1910. [[CrossRef](#)]
9. Bottoms, B.; Potra, A.; Samuelsen, J.R.; Schutter, S.R. Geochemical investigations of the Woodford-Chattanooga and Fayetteville Shales: Implications for genesis of the Mississippi Valley-type zinc-lead ores in the southern Ozark region and hydrocarbon exploration. *Am. Assoc. Pet. Geol. Bull.* **2019**, *103*, 1745–1768. [[CrossRef](#)]
10. Simbo, C.W.; Potra, A.; Samuelsen, J.R. A geochemical evaluation of the genetic relationship between Ouachita Mountains Paleozoic rocks and the Mississippi Valley-type mineralization in the southern Ozark Region, USA. *Ore Geol. Rev.* **2019**, *112*, 1–18. [[CrossRef](#)]
11. Philbrick, J.; Pollock, E.; Potra, A. Comparison of Elemental Geochemistry of the Arkansas Novaculite and the Boone Chert in their Type Regions, Arkansas. *J. Arkansas Acad. Sci.* **2016**, *70*, 31.
12. McKim, S.; McFarlin, F.; Chick, J.T.; Cains, J.M.; Potra, A. Textural and compositional comparison of Lower Ordovician (Cotter) and Lower Mississippian (Bone) cherts with the Arkansas Novaculite (Devonian-Mississippian), Arkansas. In *Abstracts with Programs*; Geological Society of America: Boulder, CO, USA, 2018; Volume 50.
13. Cains, J.M.; Potra, A.; Pollock, E.D. Lower Mississippian Chert Development, Southern Midcontinent Region. *J. Arkansas Acad. Sci.* **2016**, *70*, 12.
14. McKim, S.; Cains, J.M.; Chick, J.T.; McFarlin, F.; Potra, A. Lithologic Stratigraphic Position, Sequence and Diagenetic History, Lower Mississippian Tripolitic Chert, Northern Arkansas and Southern Missouri. *J. Arkansas Acad. Sci.* **2017**, *71*, 28.
15. Tosdal, R.M.; Wooden, J.L.; Bouse, R.M. Pb isotopes, ore deposits, and metallogenic terranes. *Rev. Econ. Geol.* **1999**, *12*, 1–28.
16. Leach, D.L.; Taylor, R.D.; Fey, D.L.; Diehl, S.F.; Saltus, R.W. *A Deposit Model for Mississippi Valley-Type Lead-Zinc Ores*; U.S. Geological Survey Scientific Investigations Report; U.S. Geological Survey: Reston, VA, USA, 2010.
17. Yardley, B.W.D. Metal concentrations in crustal fluids and their relationships to ore formation. *Econ. Geol. Bull. Soc. Econ. Geol.* **2005**, *100*, 613–632. [[CrossRef](#)]
18. Henley, R.W.; Truesdell, A.H.; Barton, P.B.; Whitney, J. Fluid-mineral equilibria in hydrothermal systems. *Rev. Econ. Geol.* **1984**, *1*, 267.
19. Bourcier, W.L.; Barnes, H.L. Ore solution chemistry VII: Stabilities of chloride and bisulfide complexes of zinc to 350 degrees C. *Econ. Geol. Bull. Soc. Econ. Geol.* **1987**, *82*, 1839–1863. [[CrossRef](#)]
20. Wood, S.A.; Crerar, D.A.; Borsik, M.P. Solubility of the assemblage pyrite-pyrrhotite-magnetite-sphalerite-galena-gold-stibnite-bismuthinite-argen- tite-molybdenite in H₂ O-NaCl-CO₂ solutions from 200 degrees to 350 degrees C degrees. *Econ. Geol. Bull. Soc Econ. Geol.* **1987**, *82*, 1864–1887. [[CrossRef](#)]
21. Michard, A. Rare earth element systematics in hydrothermal fluids. *Geochim. Cosmochim. Acta* **1989**, *53*, 745–750. [[CrossRef](#)]
22. Price, R.C.; Gray, C.M.; Wilson, R.E.; Frey, F.A.; Taylor, S.R. The effects of weathering on rare-earth element, Y and Ba abundances in Tertiary basalts from southeastern Australia. *Chem. Geol.* **1991**, *93*, 245–265. [[CrossRef](#)]
23. Samson, I.M.; Wood, S.A.; Finucane, K. Fluid inclusion characteristics and genesis of the fluorite-parisite mineralization in the Snowbird deposit, Montana. *Econ. Geol. Bull. Soc. Econ. Geol.* **2004**, *99*, 1727–1744. [[CrossRef](#)]
24. Tostevin, R.; Shields, G.A.; Tarbuck, G.M.; He, T.; Clarkson, M.O.; Wood, R.A. Effective use of cerium anomalies as a redox proxy in carbonate-dominated marine settings. *Chem. Geol.* **2016**, *328*, 146–162. [[CrossRef](#)]
25. Elderfield, H.; Greaves, M.J. The rare earth elements in seawater. *Nature* **1982**, *296*, 214–219. [[CrossRef](#)]
26. Johannesson, K.H.; Stetzenbach, K.J.; Hodge, V.F. Rare earth elements as geochemical tracers of regional groundwater mixing. *Geochim. Cosmochim. Acta* **1997**, *61*, 3605–3618. [[CrossRef](#)]
27. Banner, J.L.; Hanson, G.N.; Meyers, W.J. Rare earth element and Nd isotopic variations in regionally extensive dolomites from the Burlington-Keokuk Formation (Mississippian): Implications for REE mobility during carbonate diagenesis. *J. Sediment. Petrol.* **1988**, *58*, 415–432.
28. Potra, A.; Garmon, W.T.; Samuelsen, J.R.; Wulff, A.; Pollock, E.D. Lead isotope trends and metal sources in the Mississippi Valley-type districts from the Midcontinent United States. *J. Geochem. Explor.* **2018**, *192*, 174–186. [[CrossRef](#)]
29. Chinn, A.A.; Konig, R.H. Stress Inferred from Calcite Twin Lamellae in Relation to Regional Structure of Northwest Arkansas. *Geol. Soc. Am. Bull.* **1973**, *84*, 3731–3736. [[CrossRef](#)]
30. McFarland, J.D. *Stratigraphic Summary of Arkansas*; Arkansas Geological Commission Information Circular 36; Arkansas Geological Survey: Little Rock, AR, USA, 2004.
31. Holland, S.M.; Patzkowsky, M.E. Sequence architecture of the Bighorn Dolomite, Wyoming, USA; transition to the Late Ordovician icehouse. *J. Sediment. Res.* **2012**, *82*, 599–615. [[CrossRef](#)]
32. He, Z.; Gregg, J.M.; Shelton, K.L.; Palmer, J.R. Sedimentary facies control of fluid flow and mineralization in Cambro-Ordovician strata, southern Missouri. *Soc. Sediment. Geol.* **1997**, *57*, 81–99.
33. Overstreet, R.B.; Oboh-Ikuenobe, F.; Gregg, J.M. Sequence stratigraphy and depositional facies of Lower Ordovician cyclic carbonate rocks, southern Missouri, U.S.A. *J. Sediment. Res.* **2003**, *73*, 421–433. [[CrossRef](#)]
34. Lumsden, D.N.; Caudle, G.C. Origin of massive dolostone: The upper Knox model. *J. Sediment. Res.* **2001**, *71*, 400–409. [[CrossRef](#)]

35. Churnet, H.G.; Misra, K.C.; Walker, K.R. Deposition and dolomitization of upper Knox carbonate sediments, Cooper Ridge District, East Tennessee. *Geol. Soc. Am. Bull.* **1982**, *93*, 76–86. [[CrossRef](#)]
36. Kesler, S.E.; Cumming, G.L.; Krstic, D.; Appold, M.S. Lead isotope geochemistry of Mississippi Valley-type deposits of the Southern Appalachians. *Econ. Geol. Bull. Soc. Econ. Geol.* **1994**, *89*, 307–321. [[CrossRef](#)]
37. Montañez, I.P. Late diagenetic dolomitization of Lower Ordovician, upper Knox carbonates; a record of the hydrodynamic evolution of the southern Appalachian Basin. *Am. Assoc. Pet. Geol. Bull.* **1994**, *78*, 1210–1239.
38. Gregg, J.M.; Shelton, K.L. Dolomitization and dolomite neomorphism in the back reef facies of the Bonnetterre and Davis formations (Cambrian), southeastern Missouri. *J. Sediment. Petrol.* **1990**, *60*, 549–562.
39. Harper, D.D.; Borrok, D.M. Dolomite fronts and associated zinc-lead mineralization, USA. *Econ. Geol. Bull. Soc. Econ. Geol.* **2007**, *102*, 1345–1352. [[CrossRef](#)]
40. Shelton, K.L.; Gregg, J.M.; Johnson, A.W. Replacement dolomites and ore sulfides as recorders of multiple fluids and fluid sources in the southeast Missouri Mississippi Valley-type district; halogen-(super 87)/(super 86)Sr-delta (super 18)O-delta (super 34)S systematics in the Bonnetterre Dolomite. *Econ. Geol. Bull. Soc. Econ. Geol.* **2009**, *104*, 733–748. [[CrossRef](#)]
41. Anderson, G.M. Some geochemical aspects of sulfide precipitation in carbonate rocks. In *International Conference on Mississippi Valley Type Lead-Zinc Deposits*; University Missouri-Rolla: Rolla, MO, USA, 1983; pp. 61–76.
42. Leach, D.L.; Bradley, D.C.; Huston, D.L.; Pisarevsky, S.A.; Taylor, R.D.; Gardoll, S.J. Sediment-hosted lead-zinc deposits in Earth history. *Econ. Geol. Bull. Soc. Econ. Geol.* **2010**, *105*, 593–625. [[CrossRef](#)]
43. Lane, H.R. The Burlington Shelf (Mississippian, North-central United States). *Geol. Palaeo* **1978**, *12*, 165–176.
44. Shelby, P.R.; Manger, W.L. Lower mississippian transgressive-regressive carbonate sequence, Southern Ozark region. In *Abstracts with Programs*; Geological Society of America: Boulder, CO, USA, 1985; Volume 17.
45. Shelby, P.R. Depositional history of the St. Joe and Boone formations in northern Arkansas. *Proc. Arkansas Acad. Sci.* **1986**, *40*, 67–71.
46. Manger, W.L.; Shelby, P.R. Natural-gas production from the Boone Formation (Lower Mississippian), northwestern Arkansas. In *Circular*; Oklahoma Geological Survey: Norman, OK, USA, 2000; Volume 101, pp. 163–169.
47. Minor, P.M. Analysis of the tripolitic chert in the Boone Formation (Lower Mississippian, Osagean), northwest Arkansas and southwestern Missouri. Master's Thesis, University of Arkansas, Fayetteville, AR, USA, 2013; 86p.
48. Manger, W.L.; Fallacaro, A.; Dunbar, N.W. Depositional setting, lithologic character, and origin of chert in the Boone Formation (Lower Mississippian), northern Arkansas. In *Abstracts with Programs*; Geological Society of America: Boulder, CO, USA, 2002; Volume 34.
49. Tarr, W.A. Silicification of erosion surfaces. *Econ. Geol. Bull. Soc. Econ. Geol.* **1926**, *21*, 511–513. [[CrossRef](#)]
50. Manger, W.L. Understanding the Mississippian system in the southern Midcontinent, Arkansas, Missouri and Oklahoma: A historical overview. In *Abstracts with Programs*; Geological Society of America: Boulder, CO, USA, 2014; Volume 46.
51. Cains, J.M.; Chick, J.T.; Kincade, S.C.; McFarlin, F.D.; McKim, S.; Potra, A. Significance of terminated and doubly terminated quartz crystals, Lower Mississippian Boone Formation, southern Ozark region, Arkansas, Oklahoma and Missouri. In *Abstracts with Programs*; Geological Society of America: Boulder, CO, USA, 2017; Volume 49.
52. Chick, J.T.; Cains, J.M.; McFarlin, F.; McKim, S.; Potra, A. Hydrothermally Emplaced, Lower Mississippian, Tripolitic Chert and Its Possible Relationship to the Tri-State Lead-Zinc Mining District. *J. Arkansas Acad. Sci.* **2017**, *71*, 29.
53. Lillie, R.J.; Nelson, K.D.; de Voogd, B.; Brewer, J.A.; Oliver, J.E.; Brown, L.D.; Kaufman, S.; Viele, G.W. Crustal structure of Ouachita Mountains, Arkansas; a model based on integration of COCORP reflection profiles and regional geophysical data. *Am. Assoc. Pet. Geol. Bull.* **1983**, *67*, 907–931.
54. Denison, R.E. Foreland structure adjacent to the Ouachita foldbelt. In *The Appalachian-Ouachita Orogen in the United States*; Geological Society of America: Boulder, CO, USA, 1989; Volume F-2, pp. 681–688.
55. Miser, H.D. *Structure and Vein Quartz of the Ouachita Mountains of Oklahoma and Arkansas*; The Geology of the Ouachita Mountains—A Symposium; Elsevier: Amsterdam, The Netherlands, 1959; pp. 30–43.
56. Cushing, E.M.; Boswell, E.H.; Hosman, R.L. *General Geology of Mississippi Embayment*; U.S. Geology Survey Professional Papers; USGS: Reston, VA, USA, 1964; 28p.
57. Goldstein, A. Cherts and novaculites of Ouachita facies [Oklahoma-Arkansas and Texas]. *Soc. Econ. Paleo Miner. Spec. Publ.* **1959**, *7*, 135–149.
58. Godo, T.J.; Li, P.; Ratchford, M.E. Exploration for the Arkansas Novaculite reservoir, in the southern Ouachita Mountains, Arkansas. In *Abstracts: Annual Meeting*; American Association of Petroleum Geologists: Tulsa, OK, USA, 2011.
59. Honess, C.W. Geology of the southern Ouachita Mountains of Oklahoma. Part I: Stratigraphy, structure, and physiographic history. *Bull. Okla. Geol. Surv.* **1923**, *32*, 278.
60. Schutter, S.R. Lead-Zinc Mineralization as an Indicator of Unconventional Resources. *Houst. Geol. Soc. Bull.* **2015**, *57*, 32–49.
61. Diehl, S.F.; Goldhaber, M.D.; Taylor, C.D.; Swolfs, H.S.; Gent, C.A. Microstructures in the Cambrian Bonnetterre Formation, Lamotte Sandstone, and basal clastic rocks of Southeast Missouri and Northeast Arkansas: Implications of regional sulfide occurrence in stylolites and extensional veinlets for ore genesis. In *Application of Structural Geology to Mineral and Energy Resources of the Central and Western United States*; USGS: Reston, VA, USA, 1992; pp. A1–A13.
62. Bradley, D.C.; Leach, D.L. Tectonic controls of Mississippi Valley-type lead-zinc mineralization in orogenic forelands. *Miner. Depos.* **2003**, *38*, 652–667. [[CrossRef](#)]

63. Houseknecht, D.W. Evolution from passive margin to foreland basin: The Atoka Formation of the Arkoma Basin, south-central U.S.A. *Special Pub. Intl. Assoc. Sediment.* **1986**, *8*, 327–345.
64. Brockie, D.C.; Hare, E.H.; Dingess, P.R. The geology and ore deposits of the Tri-State District of Missouri, Kansas, and Oklahoma. In *The Ore Deposits of the United States, 1933–1967 (Graton-Sales Volume)*; Ridge, J.D., Ed.; The American Institute of Mining, Metallurgical, and Petroleum Engineers: New York, NY, USA, 1968; Volume 1, pp. 400–430.
65. McKnight, E.T.; Fischer, R.P. *Geology and Ore Deposits of the Picher Field, Oklahoma and Kansas*; U. S. Geology Survey Professional Paper; USGS: Reston, VA, USA, 1970; Volume 165.
66. Brannon, J.C.; Cole, S.C.; Podosek, F.A.; Ragan, V.M.; Coveney, R.M.; Wallace, M.W.; Bradley, A.J. Th-Pb and U-Pb dating of ore-stage calcite and Paleozoic fluid flow. *Science* **1996**, *271*, 491–493. [[CrossRef](#)]
67. McKnight, E.T. *Zinc and Lead Deposits of Northern Arkansas*; U. S. Geology Survey Bulletin; USGS: Reston, VA, USA, 1935; Volume 853.
68. Wenz, Z.J.; Appold, M.S.; Shelton, K.L.; Tesfaye, S. Geochemistry of Mississippi Valley-type mineralizing fluids of the Ozark Plateaus: A regional synthesis. *Am. J. Sci.* **2012**, *312*, 22–80. [[CrossRef](#)]
69. Pan, H.; Symons, D.T.A.; Sangster, D.F. Paleomagnetism of the Mississippi Valley-type ores and host rocks in the northern Arkansas and Tri-State districts. *Canad. J. Earth Sci.* **1990**, *27*, 923–931. [[CrossRef](#)]
70. Kamenov, G.D.; Mueller, P.A.; Perfit, M.R. Optimization of mixed Pb–Tl solutions for high precision isotopic analyses by MC-ICP-MS. *J. Anal. At. Spectrom.* **2004**, *19*, 1262–1267. [[CrossRef](#)]
71. Todt, W.; Cliff, R.A.; Hanser, A.; Hofmann, A.W. Evaluation of a (super 202) Pb- (super 205) Pb double spike for high-precision lead isotope analysis. *Geophys. Monogr.* **1996**, *95*, 429–437.
72. Condie, K.C. Chemical composition and evolution of the upper continental crust: Contrasting results from surface samples and shales. *Chem. Geol.* **1993**, *104*, 1–37. [[CrossRef](#)]
73. Bau, M.; Schmidt, K.; Koschinsky, A.; Hein, J.; Kuhn, T.; Usui, A. Discriminating between different genetic types of marine ferro-manganese crusts and nodules based on rare earth elements and yttrium. *Chem. Geol.* **2014**, *381*, 1–9. [[CrossRef](#)]
74. Bau, M.; Dulski, P. Distribution of yttrium and rare-earth elements in the Penge and Kuruman iron-formations, Transvaal Supergroup, South Africa. *Precambrian Res.* **1996**, *79*, 37–55. [[CrossRef](#)]
75. Möller, P.; Dulski, P.; Bau, M. Rare-earth element adsorption in a seawater profile above the East Pacific Rise. *Chem. Erde* **1994**, *54*, 129–149.
76. Bau, M.; Dulski, P.; Möller, P. Yttrium and holmium in South Pacific seawater: Vertical distribution and possible fractionation mechanisms. *Chem. Erde* **1995**, *55*, 1–15.
77. Bau, M.; Dulski, P. Comprising yttrium and rare earths in hydrothermal fluids from the Mid-Atlantic Ridge: Implications for Y and REE behaviour during near-vent mixing and for the Y/Ho ratio of Proterozoic seawater. *Chem. Geol.* **1999**, *155*, 77–90. [[CrossRef](#)]
78. Bau, M.; Koschinsky, A.; Dulski, P.; Hein, J. Comparison of the partitioning behaviours of yttrium, rare earth elements, and titanium between hydrogenetic marine ferromanganese crusts and seawater. *Geochim. Cosmochim. Acta* **1996**, *60*, 1709–1725. [[CrossRef](#)]
79. Garnit, H.; Bouhleb, S.; Barca, D.; Chtara, C. Application of LA-ICP-MS to sedimentary phosphatic particles from Tunisian phosphorite deposits: Insights from trace elements and REE into paleo-depositional environments. *Chem. Erde* **2012**, *72*, 127–139. [[CrossRef](#)]
80. Potra, A.; Moyers, A. Constraints on the sources of ore metals in Mississippi Valley-type deposits in central and east Tennessee, USA, using Pb isotopes. *Ore Geol. Rev.* **2017**, *81*, 201–210. [[CrossRef](#)]
81. Zartman, R.E.; Doe, B.R. Plumbotectonics: The model. *Tectonophysics* **1981**, *75*, 135–162. [[CrossRef](#)]
82. Piper, D.Z. Rare earth elements in ferromanganese nodules and other marine phases. *Geochim. Cosmochim. Acta* **1974**, *38*, 1007–1022. [[CrossRef](#)]
83. Piepgras, D.J.; Wasserburg, G.J. Neodymium isotopic variations in seawater. *Earth Planet. Sci. Lett.* **1980**, *50*, 128–138. [[CrossRef](#)]
84. Goldstein, S.J.; Jacobsen, S.B. The Nd and Sr systematics of riverwater dissolved material: Implications for the source of Nd and Sr in seawater. *Chem. Geol.* **1987**, *66*, 245–272.
85. Shaw, H.F.; Wasserburg, G.J. Sm-Nd in marine carbonates and phosphates: Implications for Nd isotopes in seawater and crustal ages. *Geochim. Cosmochim. Acta* **1985**, *49*, 503–518. [[CrossRef](#)]
86. Palmer, M.R. Rare Earth Elements in foraminifera tests. *Earth Planet. Sci. Lett.* **1985**, *73*, 285–298. [[CrossRef](#)]
87. Elderfield, H.; Pagett, R. Rare earth elements in ichthyoliths: Variations with redox conditions and depositional environments. *Sci. Total Environ.* **1986**, *49*, 175–197. [[CrossRef](#)]
88. Meyer, E.E.; Quicksall, A.N.; Landis, J.D.; Link, P.K.; Bostick, B.C. Trace and rare earth elemental investigation of a Sturtian cap carbonate, Pocatello, Idaho: Evidence for ocean redox conditions before and during carbonate deposition. *Precambrian Res.* **2012**, *192–195*, 89–106. [[CrossRef](#)]
89. MacRae, N.D.; Nesbitt, H.W.; Kronberg, B.I. Development of a positive Eu anomaly during diagenesis. *Earth Planet. Sci. Lett.* **1992**, *109*, 585–591. [[CrossRef](#)]
90. Sverjensky, D.A. Europium redox equilibria in aqueous solutions. *Earth Planet. Sci. Lett.* **1984**, *67*, 70–79. [[CrossRef](#)]
91. Taylor, S.R.; McLennan, S.M. The composition and evolution of the continental crust: Rare earth element evidence from sedimentary rocks. *Phil. Trans. R. Soc. Lond.* **1981**, *301*, 381–399.

92. Niem, A.R. Mississippian pyroclastic flow and ash-fall deposits in the deep-marine Ouachita flysch basin, Oklahoma and Arkansas. *Geol. Soc. Am. Bull.* **1977**, *88*, 49–61. [[CrossRef](#)]
93. Nier, A.O. Variations in the relative abundances of the isotopes of common lead from various sources. *J. Am. Chem. Soc.* **1938**, *60*, 1571–1576. [[CrossRef](#)]
94. Anderson, W.H. *Mineralization and Hydrocarbon Emplacement in the Cambrian-Ordovician Mascot Dolomite of the Knox Group in South-Central Kentucky*; Report of Investigations 4; Kentucky Geological Survey: Lexington, KY, USA, 1991; pp. 1–31.
95. Bickford, M.E.; Sides, J.R.; Cullers, R.L. Chemical evolution of magmas in the Proterozoic terrane of the St. Francois Mountains, southeastern Missouri: 1. Field, petrographic, and major element data. *J. Geophys. Res.* **1981**, *86*, 10365–10386. [[CrossRef](#)]
96. Kisvarsanyi, E.B. *General Features of the St. Francois and Spavinaw Granite-Rhyolite Terranes and the Precambrian Metallogenic Region of Southeast Missouri*; U.S. Geology Survey Bulletin; USGS: Reston, VA, USA, 1990; Volume 1932, pp. 48–57.
97. Clendenin, C.W.; Duane, M.J. Focused fluid flow and Ozark Mississippi Valley-type deposits. *Geology* **1990**, *18*, 116–119. [[CrossRef](#)]
98. Appold, M.S.; Numelin, T.J.; Shepherd, T.J.; Chenery, S.R. Limits on the metal content of fluid inclusions in gangue minerals from the Viburnum Trend, southeast Missouri, determined by laser ablation ICP-MS. *Econ. Geol. Bull. Soc. Econ. Geol.* **2004**, *99*, 185–198.
99. Gregg, J.M.; Shelton, K.L. Mississippi Valley-type mineralization and ore deposits in the Cambrian-Ordovician great American carbonate bank. *Am. Assoc. Pet. Geol. Memoir* **2012**, *98*, 161–186.
100. Erel, Y.; Listovsky, N.; Matthews, A.; Ilani, S.; Avni, Y. Tracing end-member fluid sources in subsurface iron mineralization and dolomitization along a proximal fault to the Dead Sea Transform. *Geochim. Cosmochim. Acta* **2006**, *70*, 5552–5570. [[CrossRef](#)]
101. Dublyansky, Y. Hydrothermal speleogenesis; its settings and peculiar features. In *Speleogenesis Evolution of Karst, Aquifers*; Klimchouk, A.B., Ford, D.C., Palmer, A.N., Dreybrodt, W., Eds.; National Speleological Society: Huntsville, AL, USA, 2000; pp. 292–297.